Weak-coupling model of spin fluctuations in the superconducting state of the layered cuprates

N. Bulut and D. J. Scalapino
Department of Physics, University of California, Santa Barbara, California 93106
(Received 1 July 1991)

Previous work on the modeling of normal-state spin fluctuations in $YBa_2Cu_3O_7$ is extended to the superconducting state. In this paper the effect of superconductivity on the spin fluctuations is approximately treated by using the BCS result for the irreducible susceptibility that enters the random-phase-approximation expression for the dynamic spin susceptibility. The resulting susceptibility is then used to calculate Cu(2) and O(2,3) Knight shifts and nuclear relaxation rates. Calculations are done using both *s*- and *d*-wave gap symmetries. A comparison of the results with the experimental NMR data on $YBa_2Cu_3O_7$ is presented.

I. INTRODUCTION

NMR measurements of nuclear relaxation rates and Knight shifts provide a microscopic probe of the low-frequency spin fluctuations on the CuO_2 sheets of the high-temperature superconductors.[1] From the Knight shifts and the anisotropy of the Cu(2) relaxation rates, a model of the hyperfine couplings has been constructed.[2] Using these couplings it has been shown that a random-phase approximation (RPA) form for the electronic spin susceptibility $\chi(\mathbf{q},\omega)$ can be adjusted to give a reasonably quantitative fit to the normal state NMR data on $YBa_2Cu_3O_7$.[3-6] Here we attempt to extend this work on the normal state to the superconducting state by including the effects of a superconducting gap and coherence factors in computing the irreducible part of the susceptibility that enters the RPA expression. This is the simplest modification one can make to the normal state theory which takes into account both the spin fluctuations and the pairing correlations. Just as in our previous RPA calculations for the normal state, we view this approach as providing an approximate framework for related experimental results to the structure of the underlying spin fluctuations. In particular, here we are interested in understanding the way in which the spin fluctuations change in the superconducting state and the effects of different gap symmetries on the Knight shifts and nuclear spin relaxation rates.[7,8] In addition, we are interested in exploring the limitations of this approach.

In Sec. II, we begin by discussing the modified RPA form which will be used to model the dynamic spin susceptibility of the superconducting state. Using this parametrized susceptibility, in Sec. III we calculate the Knight shifts for *s*- and *d*-wave gaps and examine the interplay of the Stoner enhancement and superconductivity. The nuclear relaxation rates for Cu(2) and O(2,3) nuclei are discussed in Sec. IV. In the one-band model that we are using, the Cu(2) and O(2,3) nuclear spins are coupled to the same susceptibility with different form factors. While the O(2,3) nuclear relaxation rate is isotropic, the Cu(2) relaxation rate is anisotropic and depends on whether the external magnetic field **H** lays in the *ab* plane or is oriented along the *c* axis, with the corresponding relaxation rates $(T_1^{-1})_{ab}$ and $(T_1^{-1})_c$, respectively. Experimentally, $(T_1^{-1})_{ab}$, $(T_1^{-1})_c$, and $(T_1^{-1})_O$ do not have Hebel-Slichter[9] peaks below T_c, but rather show a rapid decrease as T drops below T_c. In addition, the observed Cu(2) anisotropy,[10,11] $(T_1^{-1})_{ab}/(T_1^{-1})_c$, and the Cu(2) to O(2,3) anisotropy ratio[12] $(T_1^{-1})_c/(T_1^{-1})_O$ exhibit unusual temperature variations as T/T_c decreases. In Sec. IV we examine this anisotropy and its possible relationship to the symmetry and magnitude of the gap. Section V contains a summary of our conclusions.

II. DYNAMIC SPIN SUSCEPTIBILITY FOR $T < T_c$

In previous work[3] on the normal state we used as RPA form for the susceptibility $\chi(\mathbf{q},\omega)$ given by

$$\chi(\mathbf{q},\omega)=\frac{\chi_0(\mathbf{q},\omega)}{1-U\chi_0(\mathbf{q},\omega)}\ , \tag{1}$$

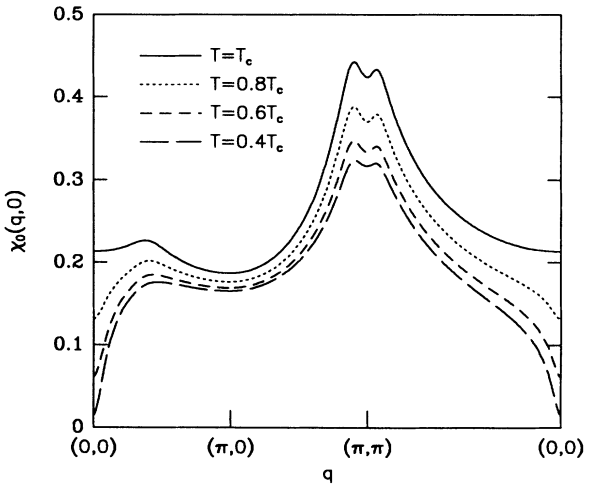

FIG. 1. Static susceptibility $\chi_0(\mathbf{q},0)$ vs $\mathbf{q}$ along a path from Γ to X to M to Γ in the Brillouin zone for an *s*-wave gap as T is lowered below T_c. Here the amplitude of the superconducting gap is $2\Delta_0=3.52kT_c$.

to describe the spin dynamics in the metallic regime of the layered cuprates. Here $\chi_0(\mathbf{q},\omega)$ is the noninteracting susceptibility and U is a reduced Coulomb repulsion, which is assumed to be renormalized due to particle-particle correlations. The strength of antiferromagnetic (AF) fluctuations required to fit the normal state NMR data was adjusted by varying U and the filling $\langle n \rangle$. In the normal state we were able to fit the data on the Cu(2) and O(2,3) relaxation rates and the Cu(2) anisotropy on $YBa_2Cu_3O_7$ by using $U=2t$ and $\langle n \rangle = 0.86$. Here we will continue to use these values for U and $\langle n \rangle$.

In order to model $\chi(\mathbf{q},\omega)$ below T_c, we use the RPA form of Eq. (1) with the irreducible BCS susceptibility $\chi_0(\mathbf{q},\omega)$ given by

$$\chi_0(\mathbf{q},\omega)=\frac{1}{N}\sum_{\mathbf{p}}\left[\frac{1}{2}\left[1+\frac{\varepsilon_{\mathbf{p}+\mathbf{q}}\varepsilon_{\mathbf{p}}+\Delta_{\mathbf{p}+\mathbf{q}}\Delta_{\mathbf{p}}}{E_{\mathbf{p}+\mathbf{q}}E_{\mathbf{p}}}\right]\frac{f(E_{\mathbf{p}+\mathbf{q}})-f(E_{\mathbf{p}})}{\omega-(E_{\mathbf{p}+\mathbf{q}}-E_{\mathbf{p}})+i\Gamma}\right.$$
$$+\frac{1}{4}\left[1-\frac{\varepsilon_{\mathbf{p}+\mathbf{q}}}{E_{\mathbf{p}+\mathbf{q}}}+\frac{\varepsilon_{\mathbf{p}}}{E_{\mathbf{p}}}-\frac{\varepsilon_{\mathbf{p}+\mathbf{q}}\varepsilon_{\mathbf{p}}+\Delta_{\mathbf{p}+\mathbf{q}}\Delta_{\mathbf{p}}}{E_{\mathbf{p}+\mathbf{q}}E_{\mathbf{p}}}\right]\frac{1-f(E_{\mathbf{p}+\mathbf{q}})-f(E_{\mathbf{p}})}{\omega+(E_{\mathbf{p}+\mathbf{q}}+E_{\mathbf{p}})+i\Gamma}$$
$$\left.+\frac{1}{4}\left[1+\frac{\varepsilon_{\mathbf{p}+\mathbf{q}}}{E_{\mathbf{p}+\mathbf{q}}}-\frac{\varepsilon_{\mathbf{p}}}{E_{\mathbf{p}}}-\frac{\varepsilon_{\mathbf{p}+\mathbf{q}}\varepsilon_{\mathbf{p}}+\Delta_{\mathbf{p}+\mathbf{q}}\Delta_{\mathbf{p}}}{E_{\mathbf{p}+\mathbf{q}}E_{\mathbf{p}}}\right]\frac{f(E_{\mathbf{p}+\mathbf{q}})+f(E_{\mathbf{p}})-1}{\omega-(E_{\mathbf{p}+\mathbf{q}}+E_{\mathbf{p}})+i\Gamma}\right]. \quad (2)$$

This expression contains the usual coherence factors which are in square brackets, the dispersion relation $E_{\mathbf{p}}=\sqrt{\varepsilon_{\mathbf{p}}^2+\Delta_{\mathbf{p}}^2}$ and $\varepsilon_{\mathbf{p}}=-2t(\cos p_x+\cos p_y)-\mu$, with μ the chemical potential and $\Delta_{\mathbf{p}}$ the gap. For the gap we will examine both an s-wave form, $\Delta_{\mathbf{p}}=\Delta_0(T)$, and a d-wave form, $\Delta_{\mathbf{p}}=[\Delta_0(T)/2](\cos p_x-\cos p_y)$, with a BCS temperature dependence for $\Delta_0(T)$. In addition, a finite broadening Γ was used to model lifetime effects and control Hebel-Slichter logarithmic divergences.[13,14] In a physical system this broadening would be due to the effects of spin fluctuations on the quasiparticle self-energy. We have taken for the superconducting transition temperature $T_c=0.1t$. At $T=0.1t$ the normal state $\chi(\mathbf{q},\omega)$ has enough AF weight to give the right magnitude for Cu(2) relaxation rates measured at about 100 K in $YBa_2Cu_3O_7$.[3]

In Fig. 1 we show the effects of an s-wave superconducting gap on $\chi_0(\mathbf{q},\omega=0)$ at temperatures below T_c. We see that an s-wave gap suppresses $\chi_0(\mathbf{q},0)$ over much of the Brillouin zone. There is a strong suppression of $\chi_0(\mathbf{q}\sim 0,0)$ for $|\mathbf{q}| \lesssim \xi_{SC}^{-1}$, where ξ_{SC} is the superconducting correlation length $\xi_{SC}=0.18\hbar v_F/\Delta$. This reflects the singlet pair formation which occurs below T_c. In addition, $\chi_0(\mathbf{q},0)$ is suppressed for $\mathbf{q}\sim\mathbf{Q}=(\pi,\pi)$ as the gap opens, which causes the AF part of the RPA susceptibility to decrease rapidly. This can be understood by realizing that if, for example, $2\Delta(0)=4kT_c$, then the smearing of the Fermi surface when the system is fully superconducting is similar to the normal state at a temperature $2\Delta(0)\sim 400$ K. Thus as T decreases below T_c and the gap opens, there is a rapid decrease in $\chi_0(\mathbf{q}\sim\mathbf{Q},0)$. Since, as discussed in Sec. IV, the spectral weight which determines the nuclear spin relaxation varies as the imaginary part of Eq. (1)

$$\left.\frac{\mathrm{Im}\chi(\mathbf{q},\omega)}{\omega}\right|_{\omega\to 0}=\frac{\mathrm{Im}\chi_0(\mathbf{q},\omega)/\omega|_{\omega\to 0}}{[1-U\chi_0(\mathbf{q},0)]^2}, \quad (3)$$

a decrease in $\chi_0(\mathbf{Q},0)$ can give rise to a significant de-

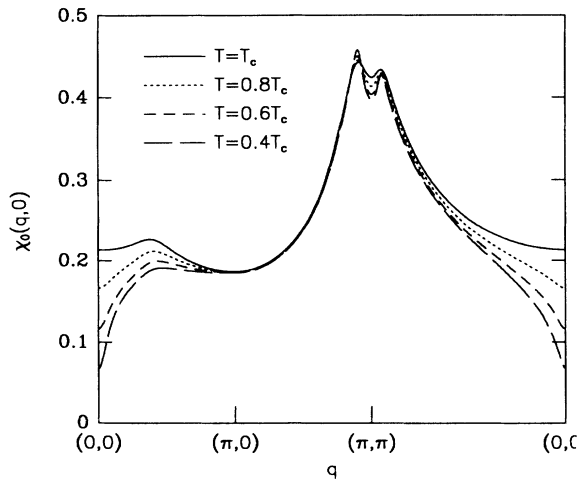

FIG. 2. Static susceptibility $\chi_0(\mathbf{q},0)$ vs $\mathbf{q}$ in the Brillouin zone for a d-wave gap as T is lowered below T_c. Here $2\Delta_0=3.52kT_c$.

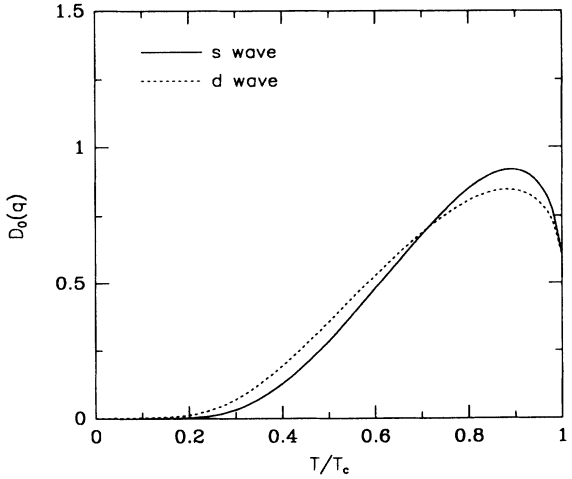

FIG. 3. $D_0(\mathbf{q})=\lim_{\omega\to 0}\mathrm{Im}\chi_0(\mathbf{q},\omega)/\omega$ vs T/T_c at $\mathbf{q}=(0.05\pi,0)$ for s- and d-wave gaps. Here $2\Delta_0=3.52kT_c$. Here and in Fig. 4 a broadening $\Gamma=0.3T_c$ has been used to control the Hebel-Slichter logarithmic singularity.

crease in the size of the antiferromagnetic spin fluctuations through the factor $[1-U\chi_0(\mathbf{q},0)]^{-2}$.

As seen in Fig. 2, for a d-wave gap the situation is different, and $\chi_0(\mathbf{q},0)$ gets suppressed only for $|\mathbf{q}| \lesssim 1/\xi_{SC}$. The lack of suppression for $\mathbf{q}\sim(\pi,\pi)$ is due to the nodes of the d-wave gap. Consequently, important AF spin fluctuations continue to exist in the d-wave superconducting state in contrast with their suppression for an s-wave gap.

As shown in Eq. (3), another factor that enters the expression for T_1^{-1} is

$$D_0(\mathbf{q})=\left.\frac{\mathrm{Im}\chi_0(\mathbf{q},\omega)}{\omega}\right|_{\omega\to 0}. \tag{4}$$

In Fig. 3 we show $D_0(\mathbf{q})$ versus T at a small wave vector $\mathbf{q}=(0.05\pi,0)$ for gaps with s- and d-wave symmetries. A similar plot is given in Fig. 4 for $\mathbf{q}\sim\mathbf{q}^*\cong(\pi,0.9\pi)$, which is in the AF region of the Brillouin zone. The wave vector $\mathbf{q}^*$ is the point where $\chi_0(\mathbf{q},0)$ peaks at low temperatures and can connect two nearly nested regions of the Fermi surface of the tight-binding model for the filling of $\langle n\rangle=0.86$. For an s-wave gap $D_0(\mathbf{q})$ has a Hebel–Slichter-like peak below T_c at both small and large wave vectors. $D_0(\mathbf{q})$ has a similar peak for a d-wave gap at $\mathbf{q}=(0.05\pi,0)$, however it is quite different at $q\sim q^*$. At this latter wave vector, $D_0(\mathbf{q})$ does not have a peak below T_c for a d-wave gap and in addition exhibits a substantial spectral weight even at low temperatures. These features arise for a d-wave gap because of the nodes on the Fermi surface and the behavior of the coherence factors.

Finally, in this section, we show the superconducting density of states

$$N_S(\omega)=\begin{cases}\dfrac{1}{N}\displaystyle\sum_{\mathbf{p}}\frac{1}{2}\left[1+\frac{\varepsilon_{\mathbf{p}}}{E_{\mathbf{p}}}\right]\delta(\omega-E_{\mathbf{p}}), & \omega>0\ ,\\ \dfrac{1}{N}\displaystyle\sum_{\mathbf{p}}\frac{1}{2}\left[1-\frac{\varepsilon_{\mathbf{p}}}{E_{\mathbf{p}}}\right]\delta(\omega-E_{\mathbf{p}}), & \omega<0\ ,\end{cases} \tag{5}$$

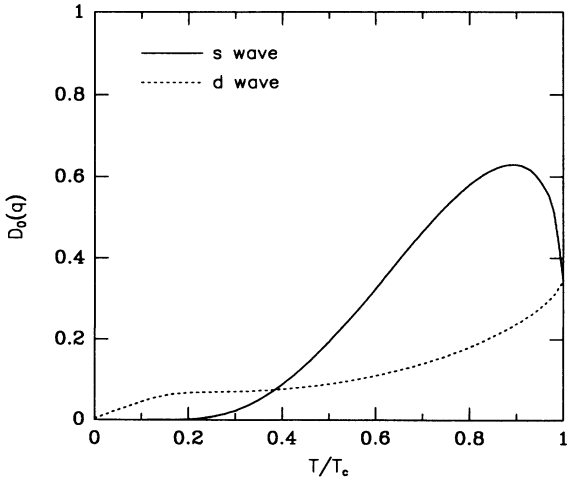

FIG. 4. $D_0(\mathbf{q})=\lim_{\omega\to 0}\mathrm{Im}\chi_0(\mathbf{q},\omega)/\omega$ vs T/T_c at $\mathbf{q}=(\pi,0.9\pi)$ for s- and d-wave gaps. Here $2\Delta_0=3.52kT_c$.

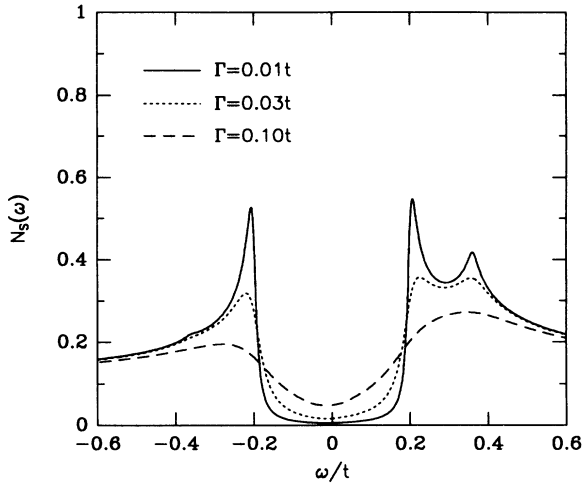

FIG. 5. Superconducting density of states $N_S(\omega)$ vs ω for $U=0$ with an s-wave gap. Here, $N_S(\omega)$ is shown for $\Delta_0=0.20t$, $\mu=-0.30t$, and difference values of Γ. At $T=0.10t$ a chemical potential of $\mu=-0.30t$ corresponds to $\langle n\rangle=0.86$.

for both s- and d-wave gaps. In Fig. 5, $N_S(\omega)$ is shown for an s-wave gap of magnitude $\Delta_0=0.2t$ and different values of the broadening parameter Γ. For $\Gamma=0$, $N_S(\omega)$ has a square-root singularity for an s-wave gap. The second peak seen for $\omega>0$ in Fig. 5 is due to the van Hove logarithmic singularity of the tight-binding model in two dimensions.

In Fig. 6, $N_S(\omega)$ is shown for a d-wave gap. A d-wave gap gives rise to a logarithmic singularity in the superconducting density of states at Δ_0 in addition to the van Hove singularity of the tight-binding model. $N_S(\omega)$ for a d-wave gap is linear in ω as $\omega\to 0$.

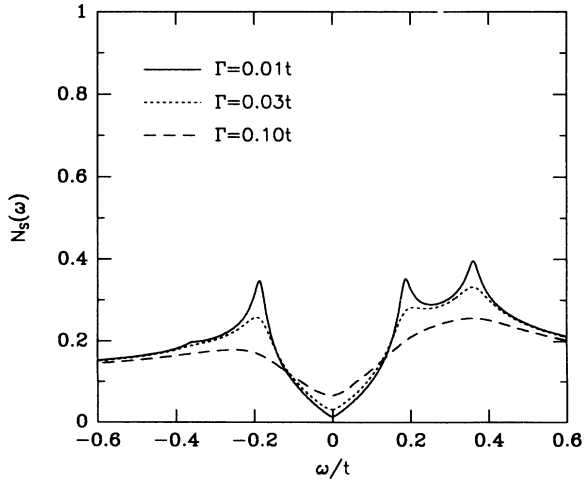

FIG. 6. Superconducting density of states $N_S(\omega)$ vs ω for $U=0$ with a d-wave gap. Here $N_S(\omega)$ is shown for $\Delta_0=0.20t$, $\mu=-0.30t$, and different values of Γ.

III. KNIGHT SHIFT

The spin contribution to the Knight shift $K_S(T)$ is proportional to $\chi(\mathbf{q}\rightarrow 0,0)$. Here we will try to fit the experimental data for the temperature dependence of the Cu(2) and O(2,3) Knight shifts by using Δ_0 as a free parameter for both s- and d-wave gaps.

First consider the case of an s-wave gap. In Fig. 7, $K_S(T)/K_S(T_c)$ versus T/T_c is plotted for $U=0$ with different gap amplitudes. This is just the well-known Yosida[15] result

$$\chi_0(\mathbf{q}\rightarrow 0,0)=-\frac{1}{N}\sum_{\mathrm{p}}\frac{\partial f(E_{\mathrm{p}})}{\partial E_{\mathrm{p}}} \tag{6}$$

for a tight-binding band. As $T\rightarrow 0$, $K_S(T)$ decays exponentially. The points in the figure are the experimental data of Takigawa *et al.*[16,17] and Barrett *et al.*[18] We see that for $U=0$, $K_S(T)$ calculated using $2\Delta_0\sim 5kT_c$ provides a reasonable fit to the data.

When the Coulomb interaction U is present, the Knight shift is proportional to

$$\chi(\mathbf{q}\rightarrow 0,0)=\frac{\chi_0(\mathbf{q}\rightarrow 0,0)}{1-U\chi_0(\mathbf{q}\rightarrow 0,0)}\ . \tag{7}$$

In Eq. (7) the Yosida function for a tight-binding band enters both the numerator and the denominator. In this case, as T decreases below T_c and χ_0 decreases, $\chi(\mathbf{q}\rightarrow 0,0)$ is further reduced by the decrease in the Stoner enhancement factor $[1-U\chi_0(0,0)]^{-1}$ in Eq. (7) for the parameters used here, $U=2t$ and $\langle n\rangle=0.86$, the Stoner enhancement in the normal state at $T=0.1t$ is 1.75. Results[19] for $U=2t$ are shown in Figs. 8(a) and 8(b). In this case the fit is good for an s-wave gap, if we use $2\Delta_0=4kT_c$.

Next we analyze the data using a d-wave gap. In Fig. 9, $K_S(T)/K_S(T_c)$ versus T/T_c is shown for $U=0$. We

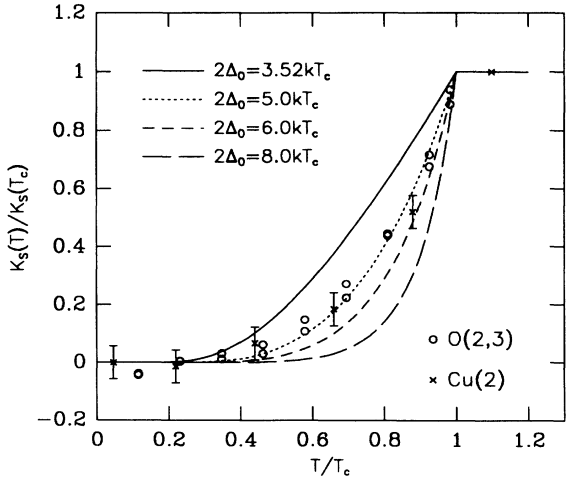

FIG. 7. Knight shift $K_S(T)/K_S(T_c)$ vs T/T_c using an s-wave gap for $U=0$ and various values of Δ_0. The points represent the experimental data by Takigawa *et al.* (Refs. 16 and 17) on O(2,3) and Barrett *et al.* (Ref. 18) on Cu(2).

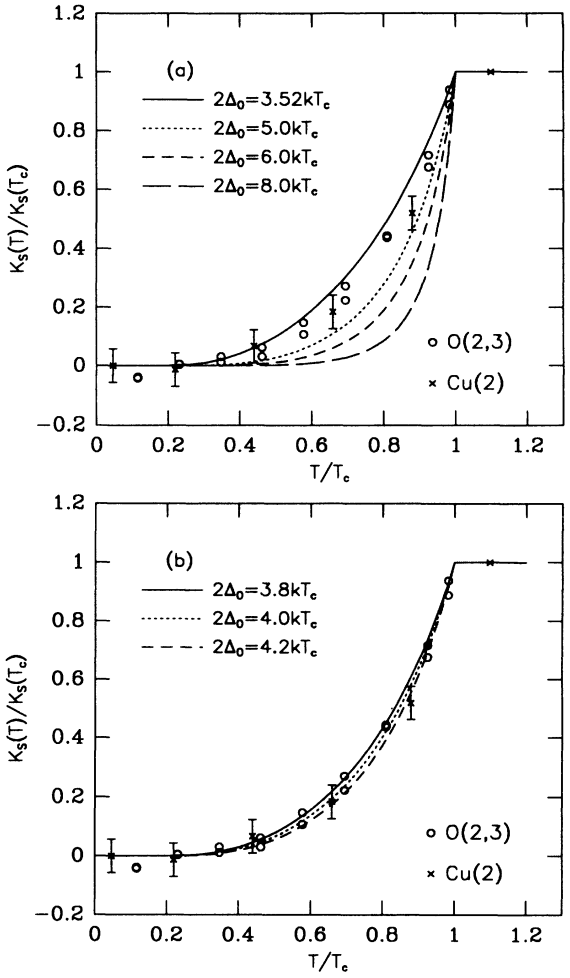

FIG. 8. Knight shift $K_S(T)/K_S(T_c)$ vs T/T_c using an s-wave gap for $U=2t$ and (a) the same values of Δ_0 as shown in Fig. 7; (b) a finer mesh of gap values near $2\Delta_0=4kT_c$. The Stoner factor for $U\neq 0$ leads to a more rapid decrease in $K_S(T)/K_S(T_c)$ for a given value of the gap so that a smaller value of $2\Delta_0$ can be used. A gap amplitude of $2\Delta_0=4kT_c$ provides a good fit to the data.

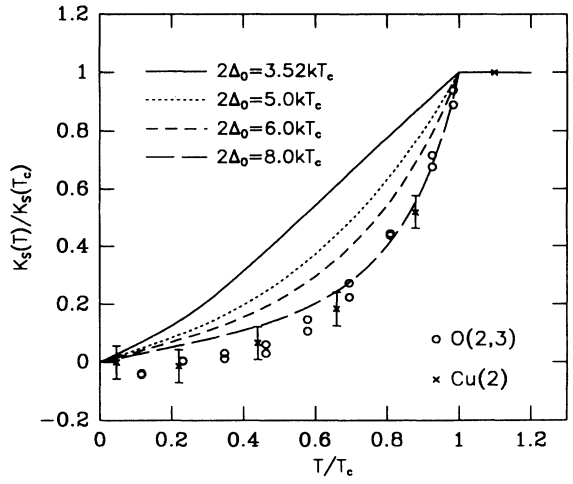

FIG. 9. Knight shift $K_S(T)/K_S(T_c)$ vs T/T_c using a d-wave gap for $U=0$ and various values of Δ_0.

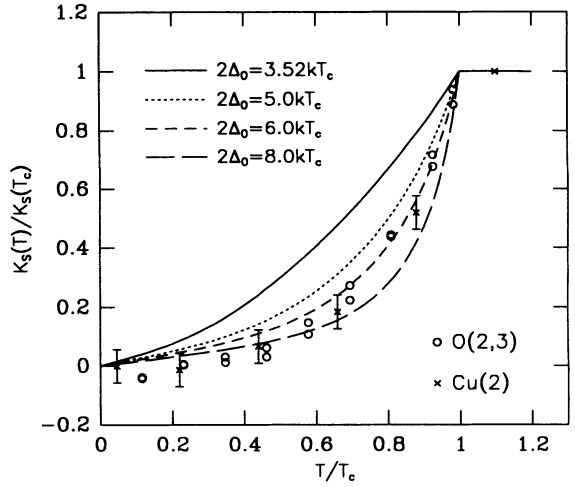

FIG. 10. Knight shift $K_S(T)/K_S(T_c)$ vs T/T_c using a d-wave gap for $U=2t$ and various values of Δ_0.

see that a gap of $2\Delta_0=8kT_c$ can fit the data for T close to T_c but fails at lower temperatures. Results with $U=2t$ are shown in Fig. 10. In this case, a gap amplitude of $2\Delta_0=6kT_c$ can fit the data near T_c. However just as for the $U=0$ results, it appears difficult to fit the data at low reduced temperatures with a d-wave gap. The experimental temperature dependence of $K_S(T)$ appears to have a vanishing slope at $T=0$. This is in contrast to the behavior of $\chi_0(\mathbf{q}\rightarrow 0,0)$ for a d-wave gap

$$\chi_0(\mathbf{q}\rightarrow 0,0)\sim 0.22\frac{k_BT}{\Delta_0}\ , \tag{8}$$

where the linear temperature dependence arises from the nodes of the d-wave gap.

In conclusion, using the modified RPA form for $\chi(\mathbf{q},\omega)$ given by Eqs. (1) and (2) with the parameters $U=2t$ and $\langle n\rangle=0.86$, which were used to fit the normal state NMR data,[3] the Knight shift data favors an s-wave gap with an amplitude $2\Delta_0$ of order $4kT_c$. However, one should keep in mind that the experimental data has error bars and K_S has been obtained by assuming a temperature independent orbital contribution to the total Knight shift. Thus the lowest temperature Cu(2) point is very important. In addition, a small error in the value of the low temperature orbital contribution for O(2,3), which shifts the zero down by less than 10%, would in fact favor a linear temperature dependence at low temperature for the O(2,3) Knight shift. Finally, throughout this work we must keep in mind that we are testing whether the simple form of $\chi(\mathbf{q},\omega)$ provided by Eqs. (1) and (2) is sufficient to provide a description of both the spin-fluctuation and pairing correlations which exist for $T<T_c$.

IV. NUCLEAR RELAXATION RATE

The nuclear relaxation rate is given, with the appropriate form factors and nuclear gyromagnetic ratios, by[20]

$$T_1^{-1}=\gamma_n^2(g\mu_B)^2\frac{k_BT}{N}\sum_{\mathbf{q}}|A(\mathbf{q})|^2\frac{\mathrm{Im}\chi(\mathbf{q},\omega)}{\omega}\bigg|_{\omega\rightarrow 0}\ . \tag{9}$$

For Cu(2) we use a hyperfine Hamiltonian, in which the Cu(2) nuclear spin has an anisotropic hyperfine coupling to the onsite Cu(2) spin and an isotropic transferred hyperfine coupling to the spins on the four neighboring Cu(2) sites. The resulting form factor depends on the orientation of the magnetic field:

$$|A_{\mathrm{Cu}}(\mathbf{q})|^2/A_{zz}^2=\begin{cases}[\frac{1}{2}(1-a_{xx})-4b\gamma_{\mathbf{q}}]^2+\frac{1}{4}(1+a_{xx})^2, & \mathbf{H}\|ab\ ,\\ (a_{xx}+4b\gamma_{\mathbf{q}})^2, & \mathbf{H}\|c\ ,\end{cases} \tag{10}$$

where $a_{xx}=A_{xx}/|A_{zz}|$, $b=B/|A_{zz}|$, and $\gamma_{\mathbf{q}}=\frac{1}{2}(\cos q_x+\cos q_y)$. For O(2,3) nuclei we assume only an isotropic transferred hyperfine coupling to the spins localized on the Cu sites. Hence, the oxygen form factor is isotropic and is given by

$$|A_{\mathrm{O}}(\mathbf{q})|^2/A_{\mathrm{O}}^2=\begin{cases}4\cos^2(q_x/2)\ ,\\ 4\cos^2(q_y/2)\ .\end{cases} \tag{11}$$

Experimentally, $K_S(T)$ with $\mathbf{H}\|c$, which is proportional to $(A_{zz}+4B)\chi(\mathbf{q}\rightarrow 0,0)$, is very small.[16–18] This requires that $b\cong 0.25$. There is experimental uncertainty in the value of a_{xx}, and we have studied values ranging from 0.4 to 0.0. Since we are only trying to fit the qualitative features of the experiments we will use $a_{xx}=0.4$.[21] Also, when we are plotting the relaxation rates, we will normalize their magnitudes by their values at T_c, hence we do not need the absolute values of A_{zz} and A_{O}.

In Fig. 11 we show the Cu(2) form factors and the O(2,3) form factor as a function of $\mathbf{q}$ in the Brillouin zone. We see that the form factor for $(T_1^{-1})_{ab}$, $|A_{ab}(\mathbf{q})|^2$, has the largest weight in the AF region of $\mathbf{q}$ space. The form factor for $(T_1^{-1})_c$, $|A_c(\mathbf{q})|^2$, has its largest weight around $\mathbf{q}\sim 0$, however it also has weight around $\mathbf{q}\sim(\pi,\pi)$, even though it is small. The form factor for $(T_1^{-1})_{\mathrm{O}}$, $|A_{\mathrm{O}}(\mathbf{q})|^2$, vanishes at $\mathbf{q}=(\pi,\pi)$ and is largest at $\mathbf{q}=(0,0)$. Thus the relaxation rate $(T_1^{-1})_{ab}$ depends most strongly on the AF fluctuations, $(T_1^{-1})_c$ experiences less of the AF fluctuations, where $(T_1^{-1})_{\mathrm{O}}$ is very weakly dependent on the AF fluctuations. This ordering of the relaxation rates according to their sensitivity to AF fluctuations will help us to understand the T_1^{-1} data for $T<T_c$.

Before presenting results for the Cu(2) and O(2,3) re-

laxation rates, we first study the relaxation rate for the $U=0$ system with an isotropic onsite hyperfine coupling A. In Fig. 12 we show T_1^{-1} versus T, for both s- and d-wave gaps with

$$(T_1^{-1})_{U=0}=\frac{T|A|^2}{N}\sum_q \frac{\mathrm{Im}\chi_0(q,\omega)}{\omega}\bigg|_{\omega\to 0}. \tag{12}$$

For an s-wave gap, T_1^{-1} exhibits the well-known Hebel-Slichter peak just below T_c, which is due to the nonvanishing coherence factors and the square-root singularity in the density of states for an s-wave gap. An approximate expression for T_1^{-1} using an s-wave gap is

$$T_1^{-1}(T)/T_1^{-1}(T_c)\sim 2f(\Delta)\left[1+\frac{\Delta}{2T}[1-f(\Delta)]\ln\frac{8\Delta}{\Gamma}\right]. \tag{13}$$

Here Γ is used to control the logarithmic singularity. As $T\to 0$, T_1^{-1} vanishes exponentially for an s-wave gap. In contrast, for $\Gamma=0.3T_c$ and a constant form factor the d-wave gap shows no Hebel-Slichter peak. Actually, for smaller values of Γ one could have a weak maximum in T_1^{-1}, but it is not singular. This is due to the fact that the singularity in the density of states, $N_S(\omega)$, for a d-wave gap is only logarithmic. At low temperatures, a d-wave gap gives a T^3 dependence for T_1^{-1}, since the density of states for a d-wave gap is linear in ω as $\omega\to 0$.

NMR experiments on $YBa_2Cu_3O_7$ in the superconducting state have produced many interesting features such as the absence of a Hebel-Slichter peak for both Cu(2) and O(2,3) relaxation rates, as well as the distinctive temperature dependences for the Cu(2) anisotropy, $(T_1^{-1})_{ab}/(T_1^{-1})_c$, and the ratio $(T_1^{-1})_c/T(_1^{-1})_O$. The points in Figs. 13(a)–13(d) show the experimental data that we will compare with our calculations. Experimentally, at low temperatures ($T\sim 30$ K) the relaxation rates depend weakly on the external magnetic field. For the Cu(2) nuclear relaxation rates $(T_1^{-1})_{ab}$ and $(T_1^{-1})_c$ we use the data obtained by Takigawa *et al.*[11] in low external magnetic field for a material which has a transition temperature of 93 K. For the O(2,3) nuclear relaxation rate $(T_1^{-1})_O$ and the ratio $(T_1^{-1})_c/(T_1^{-1})_O$ we will use the data obtained in a magnetic field of 8 T.[12] With this value of the magnetic field the superconducting transition occurs at $T=86$ K. In Fig. 13(c) we see that the Cu(2) anisotropy is of order 3.7 at $T=T_c$ and drops rapidly to values less than 3 as T decreases below T_c. At still lower temperatures it starts to increase and becomes of order 5 at $0.3T_c$. Meanwhile $(T_1^{-1})_c/(T_1^{-1})_O$ stays nearly constant with only small temperature variations [Fig. 13(d)]. Here we will vary the gap amplitude Δ_0 and the effective damping Γ, in order to explore the possibility of fitting these experimental observations using both s- and d-wave gaps. Our intention is to see what type of gap symmetry and amplitude the experimental data suggests.

We first do the analysis using an s-wave gap. In Figs. 13(a)–13(d) we show the nuclear relaxation rates $(T_1^{-1})_c$ and $(T_1^{-1})_O$, the Cu(2) anisotropy $(T_1^{-1})_{ab}/(T_1^{-1})_c$, and the ratio $(T_1^{-1})_c/(T_1^{-1})_O$ for the $U=0$ system using a BCS gap of $2\Delta_0=3.52T_c$ and a modest broadening of $\Gamma=0.3T_c$. We see that both Cu(2) and O(2,3) relaxation rates have Hebel-Slichter peaks. The calculated Cu(2) anisotropy is about 1.7 at $T=T_c$ and stays constant down to $T=0$, in spite of the fact that $(T_1^{-1})_{ab}$ and $(T_1^{-1})_c$ decrease by many orders of magnitude. $(T_1^{-1})_c/(T_1^{-1})_O$ also remains nearly constant below T_c.

In Figs. 14(a)–14(d), the same set of plots are shown for $U=2t$. At $T=T_c=0.1t$ this value of U provides an RPA enhancement of about 12.0, 5.25, and 3.75 for the relaxation rates $(T_1^{-1})_{ab}$, $(T_1^{-1})_c$, and $(T_1^{-1})_O$, respectively. Turning on U helps reduce the Hebel-Slichter

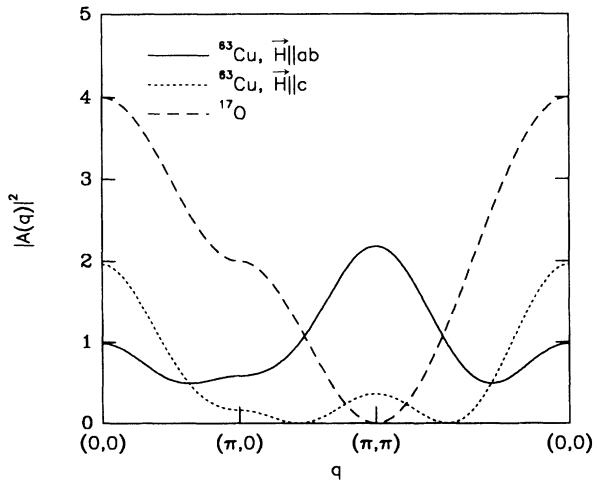

FIG. 11. The Cu(2) form factors $|A_{ab}(\mathbf{q})|^2/A_{zz}^2$ and $|A_c(\mathbf{q})|^2/A_{xx}^2$, and the O(2,3) form factor $|A_O(\mathbf{q})|^2/A_O^2$ vs $\mathbf{q}$ for the same path in the Brillouin zone as used in Fig. 1. Throughout this paper we have set $a_{xx}=A_{xx}/|A_{zz}|=0.4$ and $b=B/|A_{zz}|=0.25$.

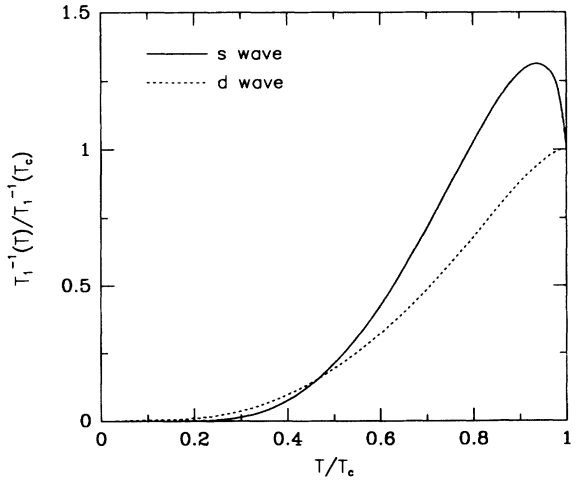

FIG. 12. The nuclear relaxation rate T_1^{-1} vs T for $U=0$ with an on-site isotropic hyperfine coupling. T_1^{-1} has been normalized by its value at $T=T_c$. Here the results are shown for both s- and d-wave gap symmetries for $2\Delta_0=3.52kT_c$ and a quasiparticle broadening $\Gamma=0.3T_c$.

peak for the Cu(2) relaxation rates since, as discussed in Sec. II, there is a rapid reduction in $[1-U\chi_0(\mathbf{q}\sim\mathbf{Q},0)]^{-2}$ as the gap opens below T_c. For O(2,3) this suppression is less pronounced, since the O(2,3) form factor filters out most of the AF fluctuations. Thus this gap amplitude and broadening are not sufficient to eliminate the Hebel-Slichter peaks completely with the biggest problem being the ^{17}O relaxation rate. Due to the loss of AF fluctuations the Cu(2) anisotropy $(T_1^{-1})_{ab}/(T_1^{-1})_c$ drops as the gap opens and stays constant once the gap saturates. In addition the experimental anisotropy has an upturn for $T<0.6T_c$. It is of course possible that as the quasiparticle excitations are frozen out another weaker magnetic relaxation mechanism with a large anisotropy becomes dominant. The ratio $(T_1^{-1})_c/(T_1^{-1})_O$ calculated using an s-wave gap also drops for $T<T_c$. This drop is similar to that found for the Cu(2) anisotropy and occurs for the same reasons. It is, however, in disagreement with the experimental data which shows little change in $(T_1^{-1})_c/(T_1^{-1})_O$ for $0.3\lesssim T/T_c\lesssim 1$. At reduced temperatures below 0.3, the rates have decreased by several orders of magnitude and other mechanisms are likely to become visible, hence we have not shown the data points taken below $T=0.3T_c$ on the plots. Here one needs to keep in mind that the experimental data on $(T_1^{-1})_c/(T_1^{-1})_O$ has been obtained in a magnetic field of

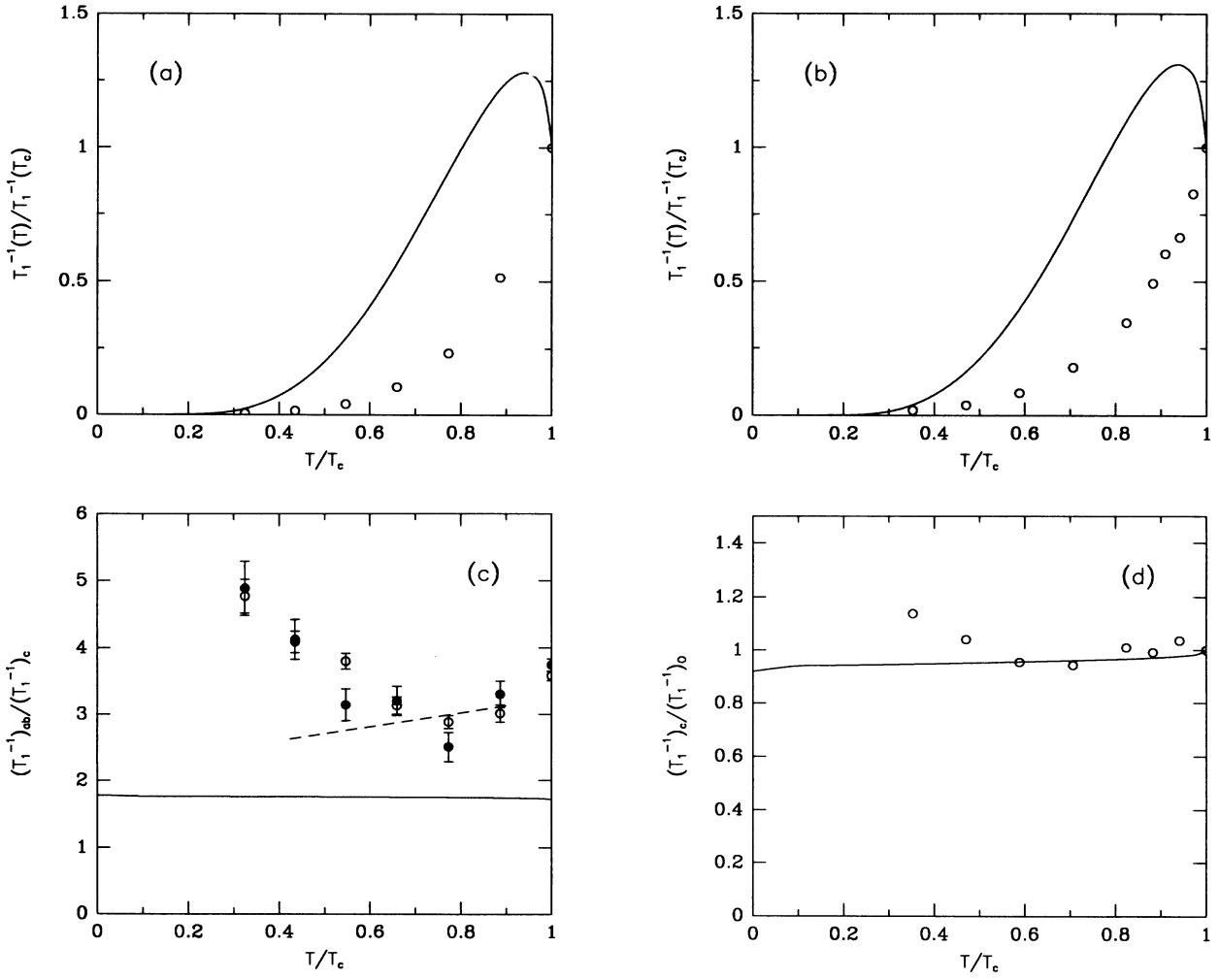

FIG. 13. Here we give results for nuclear relaxation times computed using an s-wave gap with $U=0$, $2\Delta_0=3.52kT_c$, and $\Gamma=0.3T_c$. (a) The temperature dependence of the Cu(2) nuclear relaxation rate with $\mathbf{H}\|c$, $(T_1^{-1})_c$. The points are experimental data (Ref. 11) measured in zero magnetic field with NQR. (b) The temperature dependence of the O(2,3) nuclear relaxation rate, $(T_1^{-1})_O$. The points are experimental NMR data (Refs. 12 and 17) measured in an external magnetic field of 8 T. (c) The temperature dependence of the Cu(2) anisotropy, $(T_1^{-1})_{ab}/(T_1^{-1})_c$. The points are the experimental data by Takigawa *et al.* (Ref. 11). The open circles represent $(T_1^{-1})_c$ data taken by NQR and $(T_1^{-1})_{ab}$ data taken by NMR in an external magnetic field of $H=0.44T$. The solid circles represent data taken by NMR in an external magnetic field of $H=0.44T$. The dashed line represents the experimental data by Barrett *et al.* (Ref. 10) taken both by NQR and in an external magnetic field. (d) The temperature dependence of the ratio $(T_1^{-1})_c/(T_1^{-1})_O$, normalized by its value at $T=T_c$. The points are experimental data (Refs. 12 and 17) measured in an 8-T magnetic field.

8 T, whereas our calculation is for the case of zero magnetic field.

As we have seen, it is possible to reduce the Hebel-Slichter peak by increasing Δ_0 so that the spin fluctuation enhancement factor $[1-U\chi_0(\mathbf{q},0)]^{-2}$ drops more rapidly below T_c. In addition, an increased broadening Γ is known to suppress the Hebel-Slichter peak. With this in mind we have tried a large s-wave gap of $2\Delta_0=8kT_c$ and a very large[22] temperature dependent broadening $\Gamma=2.5T_c(T/T_c)^3$. This type of temperature dependence for Γ has been previously used[13,14] and reflects the idea that as an s-wave gap starts to open the thermally excited AF spin fluctuations which are responsible for the damping will decrease. The results are shown in Figs. 15(a)–15(e). With these large values for Δ_0 and Γ, the Hebel-Slichter peaks are eliminated from both the Cu(2) and the O(2,3) relaxation rates, even though the fits to the experimental data are not particularly good. The Cu(2) anisotropy falls rapidly and then stays constant below T_c and $(T_1^{-1})_c/(T_1^{-1})_O$ has a similar temperature dependence. Both of these reflect the sudden loss of AF fluctuations for an s-wave gap below T_c. Within the model we are using, the explanation of the upturn in Cu(2) anisotropy below $T<0.6T_c$ requires an additional relaxation mechanism and the T dependence of the ratio $(T_1^{-1})_c/(T_1^{-1})_O$ is in disagreement with experiment. Figure 15(e) shows the T dependence of $(T_1^{-1})_c$ on a logarithmic scale (solid line). The exponential decay of $(T_1^{-1})_c$ at low T for an s-wave gap lies below the measured values which appear to vary more like T^3 at low temperatures. Note that Takigawa *et al.*[11] have recently confirmed that the nuclear relaxation above 30 K, corresponding to essentially all of the data shown in Fig. 15(e), is produced by magnetic processes while quadrupolar processes become significant at lower temperatures. Thus, there are a number of problems in fitting the relaxation rates with an s-wave gap. We see that even though it is possible to eliminate the Hebel-Slichter peaks in the relaxation rates using an s-wave gap with large values of Δ_0 and Γ, fitting the detailed temperature dependences of the data with a single s-wave gap is difficult.

Next we analyze the experimental data using a d-wave gap. Just as for the previous case of an s-wave gap, it is instructive to begin by considering the effect of a d-wave

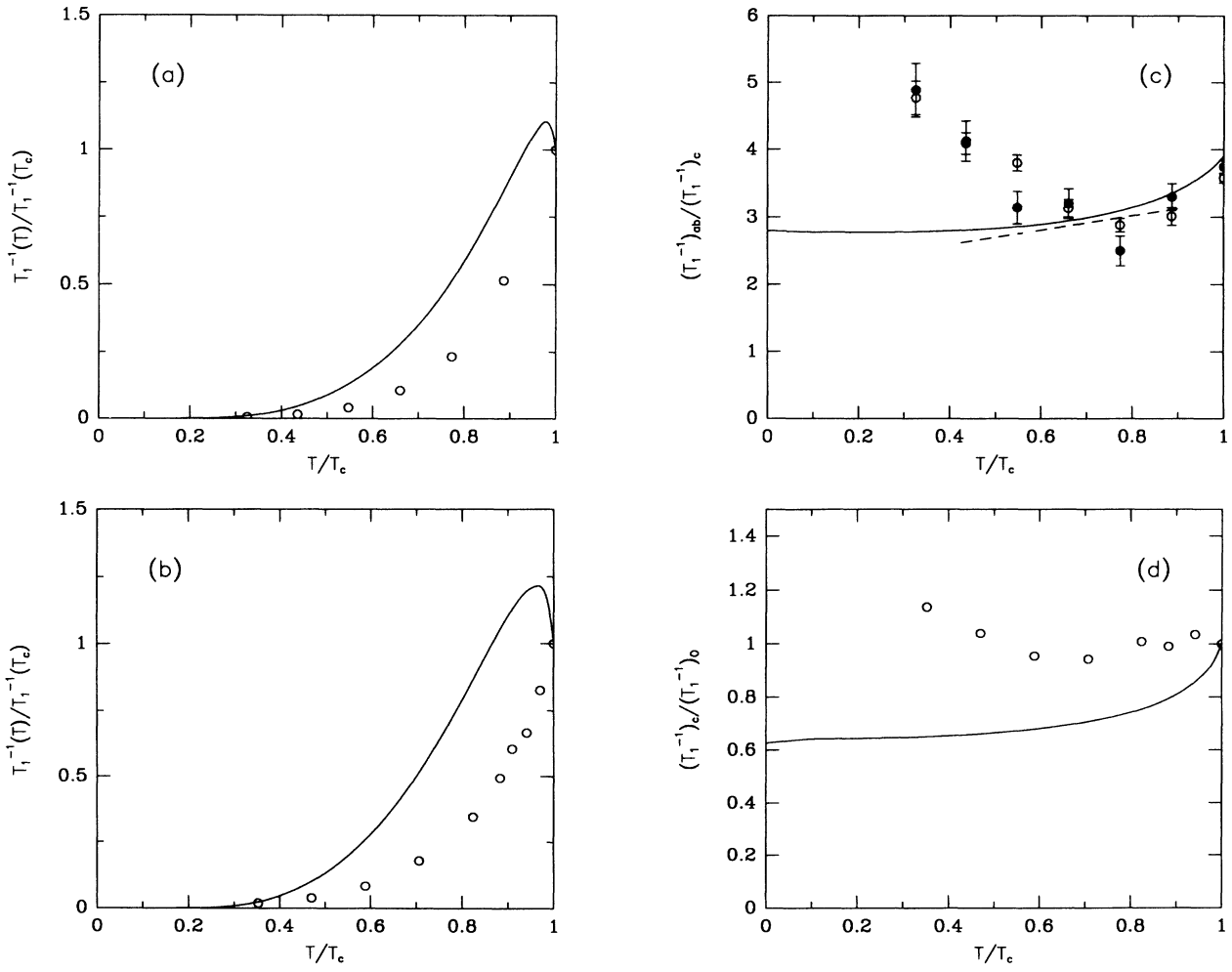

FIG. 14. Similar results to those shown in Fig. 13 with $U=2t$ for an s-wave gap with $2\Delta_0=3.52kT_c$ and $\Gamma=0.3T_c$.

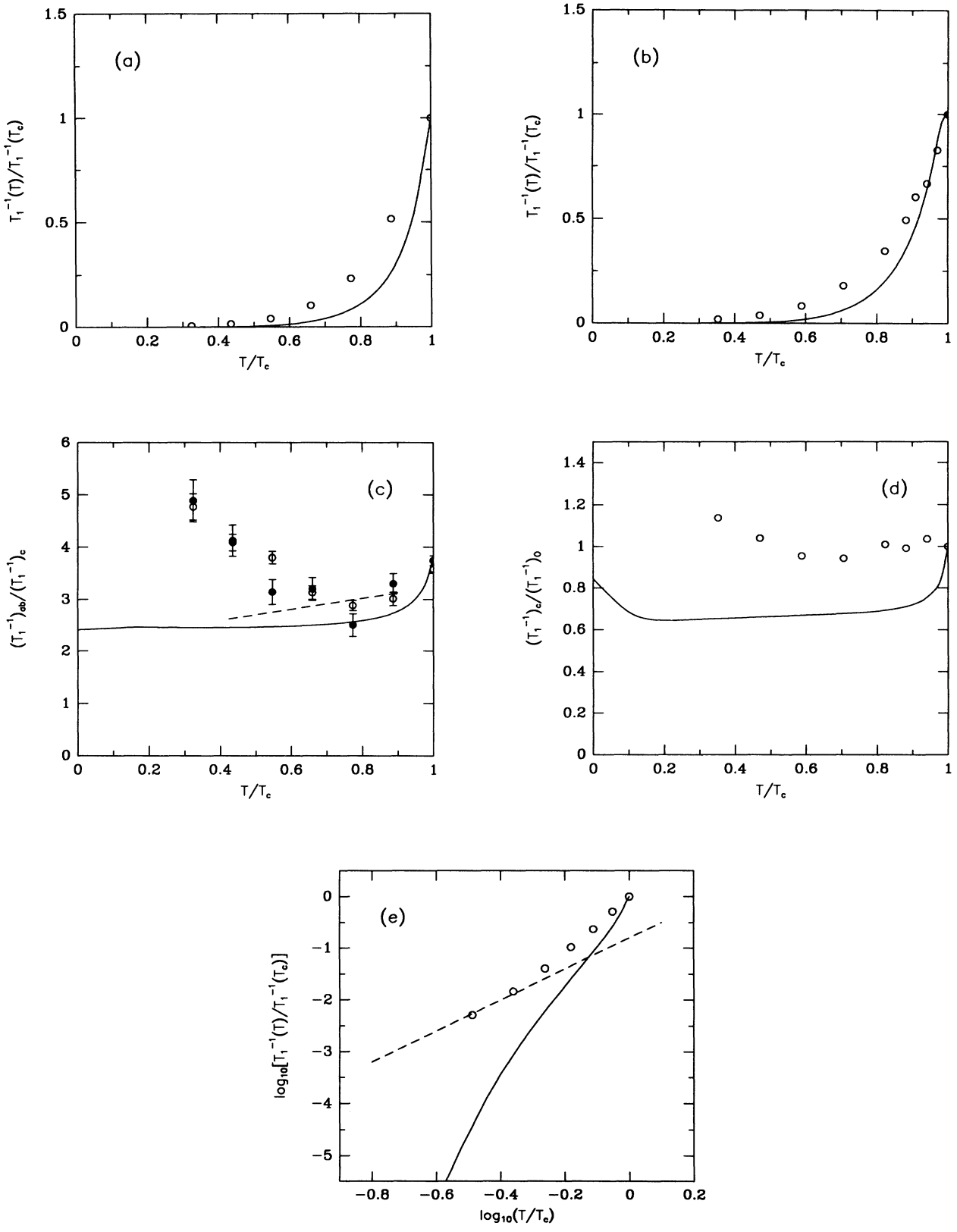

FIG. 15. Similar results to those shown in Fig. 13 with $U=2t$ for an s-wave gap with $2\Delta_0=8kT_c$ and $\Gamma=2.5T_c(T/T_c)^3$. Here (e) shows $\log_{10}[T_1^{-1}(T)/T_1^{-1}(T_c)]$ vs $\log_{10}(T/T_c)$ for the Cu(2) relaxation rate with $\mathbf{H}\|c$ (solid line). The open circles represent the data taken with NQR (Ref. 11). The dashed line has a slope of three.

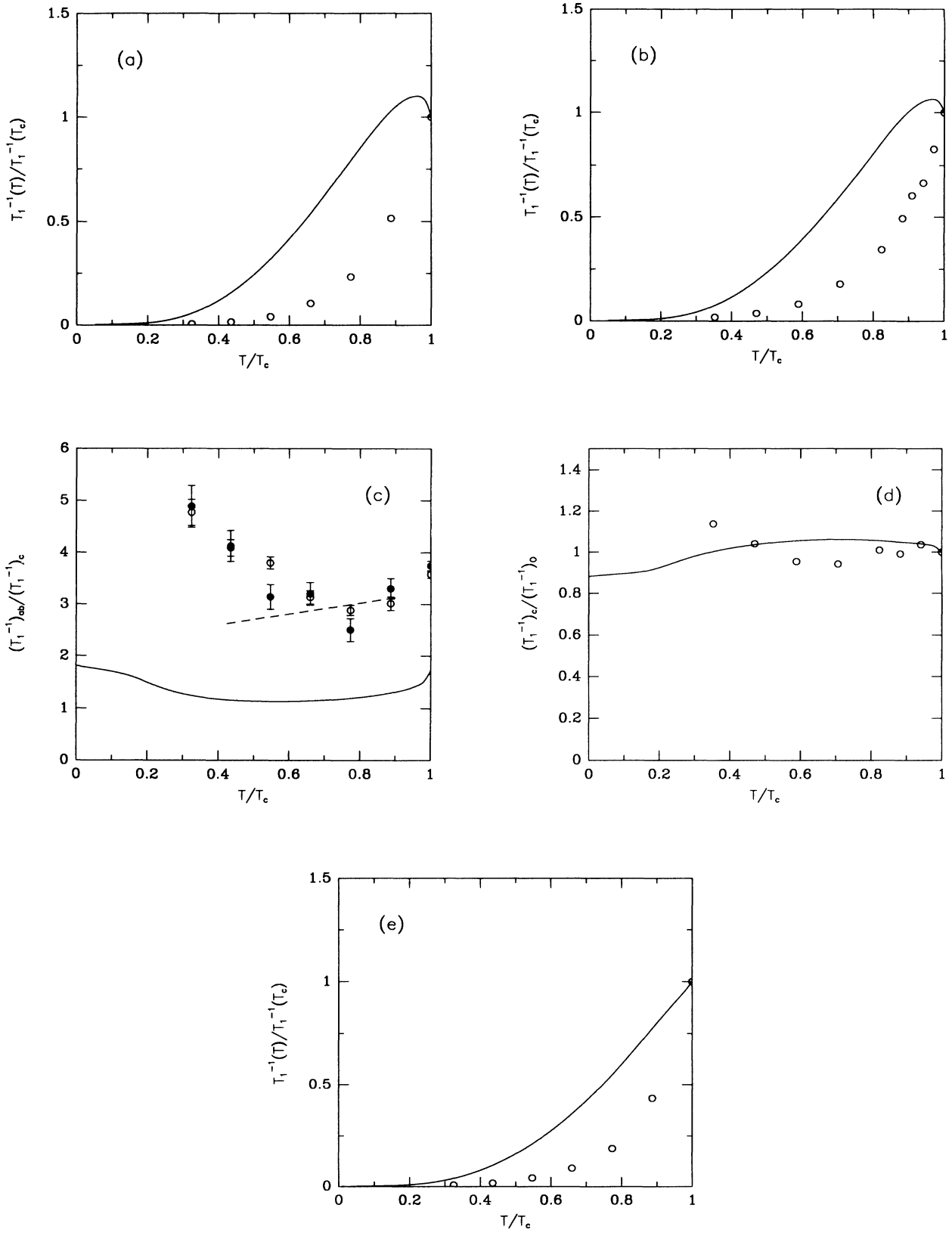

FIG. 16. Similar results to those shown in Fig. 13 with $U=0$ and a d-wave gap with $2\Delta_0=3.52kT_c$ and $\Gamma=0.3T_c$. Here (e) shows the temperature dependence of the Cu(2) nuclear relaxation rate with $\mathbf{H}\|ab, T(T_1^{-1})_{ab}$. The open circles represent the data on $(T_1^{-1})_{ab}$ measured in a low external magnetic field (Ref. 11).

gap when $U=0$ and there is no Coulomb enhancement of the spin fluctuations. Then following this, we will examine the behavior when $U=2t$. In Figs. 16(a)–16(e) we show a set of plots with $U=0$ for a d-wave gap with $2\Delta_0=3.52kT_c$ and a broadening of $\Gamma=0.3T_c$. As shown in Figs. 3 and 4, $D_0[\mathbf{q}\sim(\pi,\pi)]$ does not peak below T_c, while $D_0(\mathbf{q}\sim 0)$ does. Thus $(T_1^{-1})_c$ and $(T_1^{-1})_O$ exhibit small peaks below T_c since their form factors have more weight around $\mathbf{q}\sim 0$ while $(T_1^{-1})_{ab}$, shown in Fig. 16(e) has no Hebel-Slichter peak because its form factor is dominated by the $\mathbf{q}=(\pi,\pi)$ region. For these same reasons $(T_1^{-1})_{ab}/(T_1^{-1})_c$ decreases below T_c while $(T_1^{-1})_c/(T_1^{-1})_O$ shows only a weak T dependence.

Results with $U=2t$, $2\Delta_0=3.52kT_c$, and $\Gamma=0.3T_c$ are shown in Figs. 17(a)–17(d). $(T_1^{-1})_c$ and $(T_1^{-1})_O$ do not decay as rapidly as the data and $(T_1^{-1})_O$ still has a small peak just below T_c. However, the similarity of the calculated Cu(2) anisotropy to the experimental data is remarkable. The calculated anisotropy first decreases from 3.8 to 2.8 as the gap opens, but for $T\lesssim 0.5T_c$ it starts to increase and reaches 5 at $T\sim 0.2T_c$. The initial drop in the anisotropy is due to the fact that $|A_{ab}(\mathbf{q})|^2$ has a larger weight around $\mathbf{q}\sim(\pi,\pi)$ than $|A_c(\mathbf{q})|^2$. Thus since $D_0[\mathbf{q}\sim(\pi,\pi)]$ decreases as T goes below T_c, whereas $D_0(\mathbf{q}\sim 0)$ has a peak, the anisotropy ratio initially decreases. However, at lower reduced temperatures, $D_0(\mathbf{q}\sim 0)$ decays faster than $D_0(\mathbf{q}\sim\mathbf{q}^*)$ because of the nodes, as discussed in Sec. II, and this causes the eventual upturn in the Cu(2) anisotropy. Within this model the structure in the Cu(2) anisotropy can be attributed to the nodes of a d-wave gap and to the behavior of the T_1^{-1} coherence factors for a gap with d-wave symmetry. For similar reasons the comparison between the calculated and the experimental $(T_1^{-1})_c/(T_1^{-1})_O$ is reasonable.

In order to remove the small peaks in $(T_1^{-1})_c$ and $(T_1^{-1})_O$ we turn on a large gap of $2\Delta_0=8kT_c$ and set $\Gamma=T_c(T/T_c)^3$. The results for this set of parameters are shown in Figs. 18(a)–18(e). We see that the temperature dependences of $(T_1^{-1})_c$, $(T_1^{-1})_O$, and $(T_1^{-1})_{ab}/(T_1^{-1})_c$ are in reasonable agreement with the experiment. However, the ratio $(T_1^{-1})_c/(T_1^{-1})_O$ dips more than the experimental results below T_c. Since our aim here is to com-

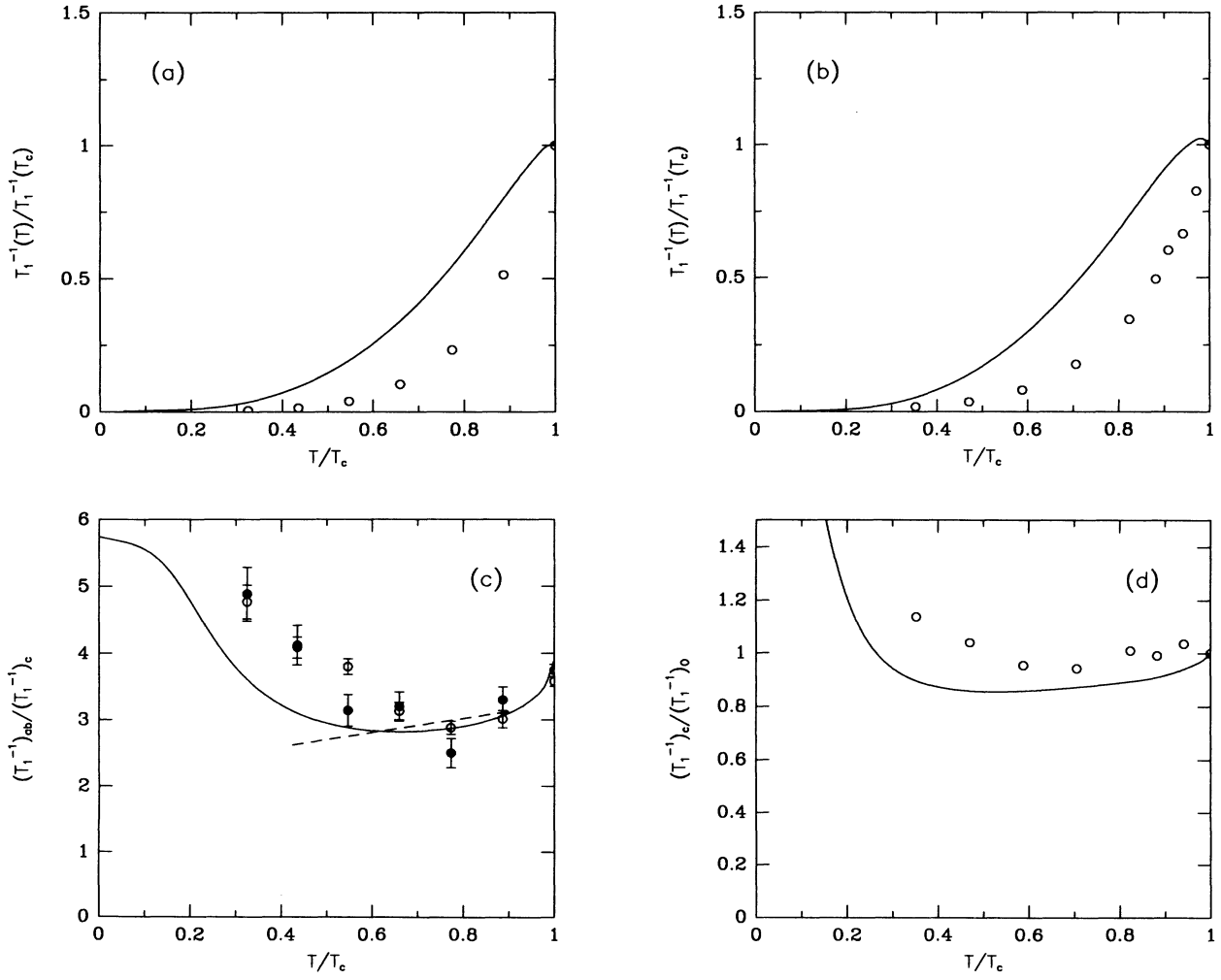

FIG. 17. Similar results to those shown in Fig. 13 with $U=2t$ and a d-wave gap with $2\Delta_0=3.52kT_c$ and $\Gamma=0.3T_c$.

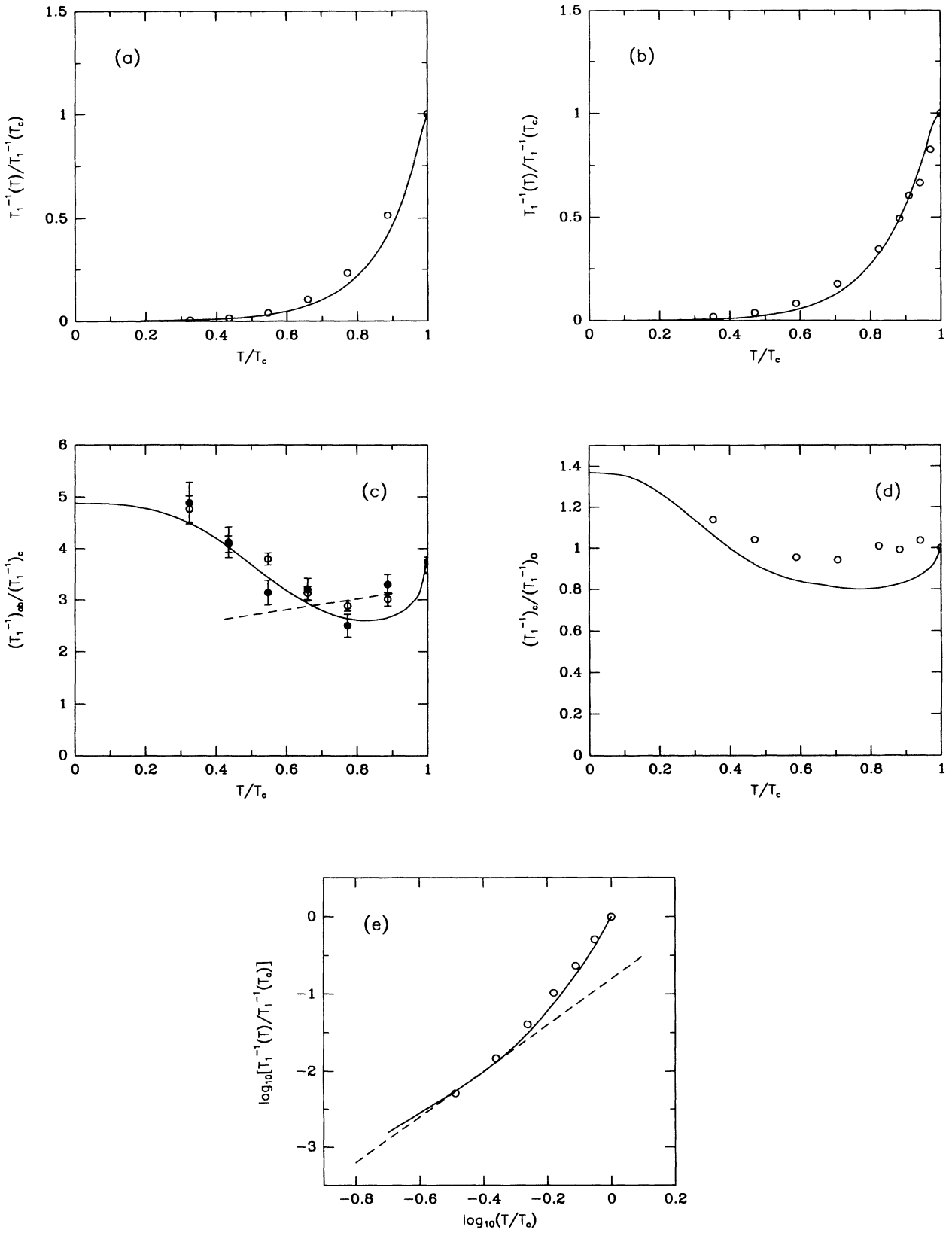

FIG. 18. Similar results to those shown in Fig. 13 with $U=2t$ and a d-wave gap with $2\Delta_0=8kT_c$ and $\Gamma=T_c(T/T_c)^3$. Here (e) shows $\log_{10}[T_1^{-1}(T)/T_1^{-1}(T_c)]$ vs $\log_{10}(T/T_c)$ for the Cu(2) relaxation rate with $\mathbf{H}\|c$ (solid line). The open circles represent the data taken with NQR (Ref. 11). The dashed line has a slope of three.

pare qualitative features rather than making quantitative fits to experiments, we have not tried further parameter variations. Figure 18(e) shows the temperature dependence of $(T_1^{-1})_c$ on a logarithmic scale. The T^3 decay of $(T_1^{-1})_c$ at low T for a d-wave gap does not require the existence of a second relaxation mechanism. Our scheme for calculating T_1^{-1} just below T_c may well be too simple, and a more sophisticated calculation might eliminate the peaks in $(T_1^{-1})_c$ and especially $(T_1^{-1})_O$ using smaller values for Δ_0 and Γ.

V. CONCLUSIONS

We have analyzed the Knight shift and T_1^{-1} data for the Cu(2) and O(2,3) nuclei in $YBa_2Cu_3O_7$ for $T<T_c$ using a weak coupling model for a metal with AF spin fluctuations. This model has been previously used to fit the normal state NMR data. The effective Coulomb interaction $U=2t$ and the average site occupancy $\langle n \rangle$ were previously fixed by fitting the normal state data. Here the correlations arising in the superconducting state were modeled by using superconducting propagators to calculate the irreducible part of the susceptibility that appears in the RPA expression for $\chi(\mathbf{q},\omega)$. Then for $T<T_c$, we considered calculations using both s- and d-wave gaps with the gap amplitude Δ_0 and the broadening Γ used as adjustable parameters.

An analysis of the Knight shift data showed that an s-wave gap with $2\Delta_0=4kT_c$ provided a satisfactory fit to data. The Coulomb repulsion of $U=2t$ that we are using in our calculations provides a Stoner enhancement of 1.75 for $K_S(T)$ at $T=T_c$. With the same Stoner enhancement a d-wave gap of order $2\Delta_0=5$ to $6kT_c$ was required to fit the initial drop in K_S near T_c. However, at low temperatures the d-wave results did not give as satisfactory a fit to the data as an s-wave gap. It is especially difficult to fit the data with a d-wave gap at low temperatures, where the data points seem to go to $T=0$ with a vanishing slope, in contrast with the linear T dependence of $K_S(T)$ for a d-wave gap at low T.

In the analysis of the T_1^{-1} data we have seen the importance of the form factors. In our model $(T_1^{-1})_{ab}$, $(T_1^{-1})_c$, and $T(T_1^{-1})_O$ sample the same susceptibility with different form factors. We have observed that $(T_1^{-1})_{ab}$ is the most sensitive to the AF spin fluctuations, $(T_1^{-1})_c$ is less sensitive to the AF fluctuations than $(T_1^{-1})_{ab}$, whereas $(T_1^{-1})_O$ is the least sensitive.

Within the framework of Eqs. (1) and (2), there are a number of difficulties in fitting the T^{-1} relaxation data with an s-wave gap. The first problem is with the Hebel-Slichter peaks which appear when an s-wave gap is used unless there is an unphysically large damping factor. In Sec. II, we have seen that when an s-wave gap opens, the RPA enhancement of the spin fluctuations is reduced. While this helps to suppress the Cu(2) Hebel-Slichter peaks in $(T_1^{-1})_{ab}$, and $(T_1^{-1})_c$, it does little to remove the peak in $(T_1^{-1})_{\parallel}$, since the oxygen form factor has already removed much of the AF spectral weight. Thus in Sec. IV, we found that even a rough fit of the T_1^{-1} data required large values of both $2\Delta_0=8kT_c$ and $\Gamma=2.5T_c(T/T_c)^3$. However, as shown in Sec. III, such a large value of $2\Delta_0$ is inconsistent with the Knight shift data. Furthermore, a $\Gamma(T_c)$ of $2.5T_c$ corresponds to a quasiparticle lifetime of $5T_c$ which is significantly larger than the value of order $2T_c$ obtained from various transport measurements.[22] In addition even when the Hebel-Slichter peaks have been eliminated using large values of Δ_0 and Γ, the temperature dependence of the Cu(2) anisotropy and the $(T_1^{-1})_c/(T_1^{-1})_O$ ratio pose problems. Since the $(T_1^{-1})_{ab}$ form factor sees more of the AF fluctuations than the $(T_1^{-1})_c$ form factor, and the AF fluctuations decrease rapidly as the s-wave gap opens, there is an initial drop in the $(T_1^{-1})_{ab}/(T_1^{-1})_c$ ratio. However, at lower temperatures, this calculated anisotropy ratio was found to remain constant. Thus, the experimentally observed upturn in anisotropy would require that a second mechanism becomes dominant for $T/T_c<0.7$. While this is certainly possible, it seems *ad hoc*. Finally, the experimental temperature independence of the ratio $(T_1^{-1})_c/(T_1^{-1})_O$ for $T<T_c$ is in disagreement with the predictions using an s-wave gap. With an s-wave gap we found that $(T_1^{-1})_c/(T_1^{-1})_O$ initially drops below T_c, due to the loss of AF fluctuations, and stays constant as T is lowered further. In view of all these difficulties we conclude that it is difficult to fit the T_1^{-1} data using an s-wave gap within the framework of our model.

On the other hand, a d-wave gap seems to yield results more consistent with the T_1^{-1} data. Using the parameters $2\Delta_0=8kT_c$ and $\Gamma=T_c(T/T_c)^3$, we have seen that $(T_1^{-1})_c$, $(T_1^{-1})_O$, and $(T_1^{-1})_{ab}/(T_1^{-1})_c$ provide reasonable fits to the experiment. The structures in $(T_1^{-1})_{ab}/(T_1^{-1})_c$ and $(T_1^{-1})_c/(T_1^{-1})_O$ arise from the nodes of a d-wave gap on the Fermi surface and do not involve a second relaxation mechanism.

Thus we are left with a puzzle. The temperature dependence of the Knight shift, as well as the magnetic penetration depth data,[23] support the view that the gap is nodeless. Yet within the framework provided by Eqs. (1) and (2) we find that it is difficult to explain the T_1^{-1} data with an s-wave gap and that a d-wave gap gives results which on the surface look more like experiment. Thus we conclude that while the RPA form provides a means of parametrizing the data on $YBa_2Cu_3O_7$ for $T>T_c$, the simple extension of it to the superconducting region $T<T_c$ fails. However, we believe it provides some interesting clues regarding the interplay of the spin-fluctuation correlations and the pairing correlations.

First, the rapid decrease of the Knight shift, which within the usual Yosida form implies a large value of $2\Delta_0(0)/kT_c$, can be obtained with a moderate sized $2\Delta_0(0)/kT_c$ when the spin-fluctuation "Stoner" enhancement is taken into account.

Second, the Hebel-Slichter peak for Cu(2) is reduced when the RPA corrections to the usual quasiparticle superconducting susceptibility are kept [compare Fig. 14(a) with Fig. 13(a)]. Thus, as suggested by Schrieffer,[24] Coulomb vertex corrections can affect the Hebel-Slichter peak. Within the RPA form these vertex corrections lead to

$$\mathrm{Im}\chi(\mathbf{q},\omega)=\frac{\mathrm{Im}\chi_0(\mathbf{q}\omega)}{[1-U\,\mathrm{Re}\chi_0(\mathbf{q},\omega)]^2+[U\,\mathrm{Im}\chi_0(\mathbf{q},\omega)]^2}\ , \tag{14}$$

so that the nuclear relaxation process can arise from antiferromagnetic fluctuations where $[1-U\,\mathrm{Re}\chi_0(\mathbf{q},0)]$ is small, as well as the usual quasiparticle spin fluctuations contained in $\mathrm{Im}\chi_0(\mathbf{q},\omega)$. It is these latter fluctuations that contain the well-known Hebel-Slichter logarithmic divergence. Unfortunately, within our present framework it is difficult to remove the influence of these quasiparticle spin fluctuations from the oxygen T_1^{-1} relaxation because its form factor suppresses the $\mathbf{q}=(\pi,\pi)$ collective antiferromagnetic fluctuations [see Figs. 13(b) and 14(b)]. Nevertheless, it appears that it will be important to understand the role of the para-antiferromagnetic spin-wave fluctuations in providing T_1^{-1} relaxation in the superconducting state.

ACKNOWLEDGMENTS

We want to thank Barrett *et al.* and Takigawa *et al.* for allowing us to use their data and discussing their measurements with us. We thank N. E. Bickers for useful discussions and numerical checks. We also acknowledge helpful discussions with J. R. Schrieffer, D. Pines, H. Monien, and A. J. Millis. Partial support for this work was provided by the Electrical Power Research Institute. Numerical computations were performed at the San Diego Supercomputer Center.

[1]For a review of the experimental NMR results on high-temperature superconductors please see the following articles and the references therein: R. E. Walstedt and W. W. Warren, Jr., Science **248**, 1082 (1990); C. H. Pennington and C. P. Slichter, in *Physical Properties of High Temperature Superconductors II,* edited by D. M. Ginsberg (World Scientific, Singapore, 1990).

[2]F. Mila and T. M. Rice, Physica (Amsterdam) **157C**, 561 (1989).

[3]N. Bulut, D. Hone, D. J. Scalapino, and N. E. Bickers, Phys. Rev. B **41**, 1797 (1990); Phys. Rev. Lett. **64**, 2723 (1990).

[4]A. J. Millis, H. Monien, and D. Pines, Phys. Rev. B **42**, 167 (1990).

[5]T. Moriya, Y. Takahashi, and K. Ueda, J. Phys. Soc. Jpn. (to be published).

[6]H. Kohno and K. Yamada (unpublished).

[7]NMR experiments for $T<T_c$ have also been analyzed by H. Monien and D. Pines, Phys. Rev. B **41**, 6297 (1990).

[8]D. J. Scalapino, in *High Temperature Superconductivity Proceedings,* edited by K. S. Bedell, D. Coffey, D. E. Meltzer, and J. R. Schrieffer (Addison-Wesley, New York, 1990), p. 314.

[9]L. C. Hebel and C. P. Slichter, Phys. Rev. **113**, 1504 (1959).

[10]S. E. Barrett, J. A. Martindale, D. J. Durand, C. H. Pennington, C. P. Slichter, T. A. Friedmann, J. P. Rice, and D. M. Ginsberg, Phys. Rev. Lett. **66**, 108 (1991).

[11]M. Takigawa, J. L. Smith, and W. L. Hults (unpublished).

[12]P. C. Hammel, M. Takigawa, R. H. Heffner, Z. Fisk, and K. C. Ott, Phys. Rev. Lett. **63**, 1992 (1989).

[13]Y. Kuroda and C. M. Varma (unpublished).

[14]L. Coffey, Phys. Rev. Lett. **64C**, 1071 (1990).

[15]K. Yosida, Phys. Rev. **110**, 769 (1958).

[16]M. Takigawa, P. C. Hammel, R. H. Heffner, and Z. Fisk, Phys. Rev. B **39**, 7371 (1989).

[17]M. Takigawa, P. C. Hammel, R. H. Heffner, Z. Fisk, K. C. Ott, and J. D. Thompson, Physica (Amsterdam) **162-164C**, 853 (1989).

[18]S. E. Barrett, D. J. Durand, C. H. Pennington, C. P. Slichter, T. A. Friedmann, J. P. Rice, and D. M.Ginsberg, Phys. Rev. B **41**, 6283 (1990).

[19]Throughout this work we have set $\langle n\rangle=0.86$.

[20]Here we give rates appropriate to a nominal spin-$\frac{1}{2}$ system.

[21]In order to get the right magnitude of the anisotropy of the Cu(2) relaxation, $(T_1^{-1})_{ab}/(T_1^{-1})_c$, at $T=T_c$, we need to use $a_{xx}\sim 0.40$ and $b\sim 0.25$. However, with these values of the hyperfine couplings $(T_1^{-1})_{ab}/(T_1^{-1})_c$ has temperature dependence above T_c and it increases by about 20% as T is lowered from $0.20t$ to $0.10t$ in the normal state.

[22]Since $\tau^{-1}(T_c)=2\Gamma(T_c)=5T_c$, this broadening is more than twice that estimated from transport experiments, see, for example, R. T. Collins, Z. Schlesinger, F. Holtzberg, P. Chandari, and C. Field, Phys. Rev. B **39**, 6571 (1989).

[23]L. Krusin-Elbaum *et al.*, Phys. Rev. Lett. **62**, 217 (1989); D. R. Harshman *et al.*, Phys. Rev. B **39**, 851 (1989).

[24]J. R. Schrieffer (private communication).